

## Analytic theory of series field coil ion diodes

C. W. Mendel, Jr.

*Sandia National Laboratories, Albuquerque, New Mexico 87185*

(Received 1 March 1982)

Ion diodes suited to inertially confined fusion research must conduct very high currents. The magnetic fields due to these currents are comparable to the fields used to provide magnetic insulation of electrons. Because these self-fields are necessarily high at the diode boundary where the power is applied, and are zero at some other part of the diode away from the power feed, these diodes have generally been treated theoretically by two-dimensional particle-in-cell computer simulations. There is a special class of ion diodes employing series magnetic field coils which can be described by a one-dimensional model. These diodes are highly amenable to treatment by analytic theory, and therefore are easily designed and scaled to multiterawatt systems. Many features of these diodes make them very attractive as drivers for inertial-confinement fusion research. Theoretical analysis of this class, including magnetic field configuration and field coil design, electron drifts, diode efficiency, and ion focusing, is presented. Also presented is analysis of a plasma-filled version which provides ion bunching and filtering of light ion species which might otherwise have detrimental effects on target experiments.

### I. INTRODUCTION

Pulsed power ion diodes have made rapid progress in the few years since their inception.<sup>1-11</sup> They have achieved high efficiency ( $\sim 50\%$ ) and have demonstrated very high power output. Nevertheless the designs used originally have met with difficulties in focusing at higher power levels. The effects which cause difficulty are self-focusing of the beams and reduction of beam kinetic energy due to net drift-region beam currents, uncertain equipotential line shapes due to virtual cathodes (i.e., cathodes due to clouds of electrons not in close proximity to a physical electrode), and lack of control of relativistic-electron drifts in the diodes. This paper describes a very simple ion-beam diode geometry which overcomes these difficulties to a large degree and which can be described by analytic theory.

The configuration described is applicable to the Ampfion series of diodes. Ampfion was originally an acronym applied to the automagnetic plasma-filled ion diode.<sup>12,13</sup> All of the theory to be presented is applicable to that particular diode, but much of the theory applies equally to the Particle Beam Fusion Accelerator-I (PBFA-I) and Hydramite hybrid diodes.<sup>14</sup> These hybrid diodes use dielectric surface ion sources<sup>9</sup> rather than initial plasma fills. Some of the theory can also be used to reach a qualitative and semiquantitative understanding of other magnetically insulated ion diodes.<sup>9-11</sup>

The plasma-filled Ampfion diode has one qualitative difference from other ion diodes in that the ion acceleration gap increases in time at a rate proportional to the diode current. This results in voltage ramping which in turn results in axial focusing (bunching) if the diode focal length is chosen properly.

Sections II and III describe the one-dimensional diode geometry, the electron drifts, and the electron losses for both the plasma-filled and hybrid diodes. Sections IV and V discuss the sheath dynamics for plasma-filled diodes, and in Sec. V the filtering of light ions for multiple ion species plasmas is calculated. In Sec. VI the scaling of plasma-filled diodes to provide the best impedance match to the pulser and the best bunching of the ion beam is calculated. In Sec. VII an example of the design of a focusing ion diode is given.

### II. ONE-DIMENSIONAL DIODE GEOMETRY

The simplest diode geometry and the one to be discussed is the strip diode (Fig. 1), i.e., a planar diode of finite width and infinite length. Extension of this analysis to a practical, focusing diode can be found in Sec. VII. The theory cannot treat end effects since they are two dimensional. If  $S$  is defined as the ratio of the diode gap  $Z$  to the diode width  $b$ , then end effects are at least of order  $S^2$  since Maxwell's equations are second order. It is there-

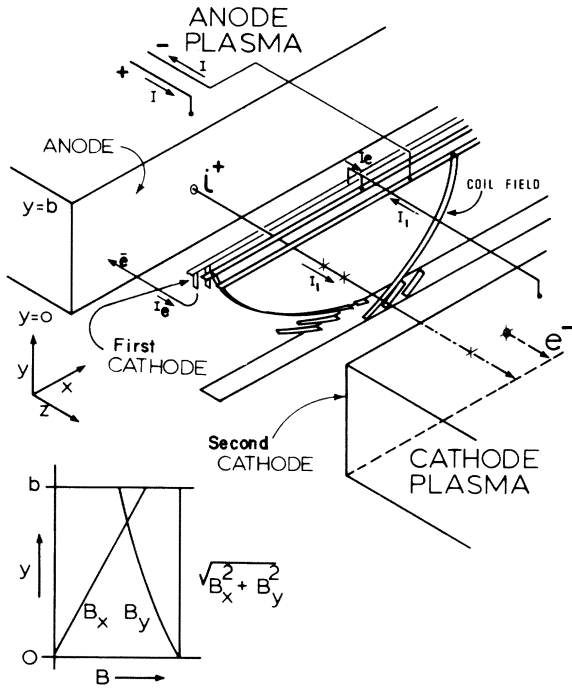


FIG. 1. Ideal strip diode. Diode extends to  $\pm\infty$  in the  $x$  direction. Figure is greatly expanded in the  $z$  direction; the separation between the anode and cathode plasmas is small in comparison to the diode height  $b$ . Pitch of the field coil varies in the  $y$  direction in such a way as to keep  $B_x^2 + B_y^2$  constant.

fore unnecessary to keep terms higher than  $S^2$ . The theory will be seen to keep second-order terms in a natural fashion.

Ion diodes suitable for inertial-confinement fusion conduct very high currents and therefore have very high self-magnetic fields (i.e., magnetic fields due to the diode current itself) at the side of the diode toward the power source. On the other side of the diode, or perhaps at some axis or plane of symmetry, the self-magnetic field must go to zero. It might seem at first glance then, that such a diode must be a two-dimensional device even when neglecting end effects. However, if the self-magnetic field is supplemented by that of a suitably designed field coil in series with the diode, the problem can be reduced to one dimension (neglecting end effects).

The geometry of such a diode may be found as follows: Assume that the electron and ion current densities to the anode are independent of  $y$  (Fig. 1) and also that the magnetic field tangential to the anode is independent of  $y$ . The latter assumption is

necessary for the electrons to gyrate with uniform radius for all values of  $y$ . This results in the tangential electron current density being independent of  $y$ . These requirements will specify the field geometry except for one parameter which may be specified as the ratio of the tangential magnetic field to the diode current. This parameter will be seen to determine the efficiency of the diode.

Since the fields are specified, the currents parallel to the anode are also specified. These currents are due to electrons drifting in the diode electric field and the tangential magnetic field. It will then be shown that the fields are indeed in the proper direction to provide the electron drifts, i.e., the fields and drifts are consistent with each other.

The magnetic field configuration will require a boundary condition which must be met by the field coil. Since the self-magnetic field is proportional to the diode current the coil field must also be proportional to the diode current and must therefore be in series with the diode to allow for time dependence.

In the following,  $J$  will be used to describe current densities to the anode whereas  $\vec{j}$  will be used for the current densities throughout the diode; also,  $Z$  will be used as the distance from anode to cathode and  $x, y, z$  will be used as the Euclidean coordinates in the diode. Subscripts  $e$  and  $i$  will refer to electron and ion parameters, respectively, and subscripts  $a$  and  $c$  will refer to anode and cathode parameters. In this section the fields will be determined in the acceleration gap as will the surface current on the anode. The details of this surface current for plasma-filled diodes will be discussed in Secs. IV and V.

The Euclidean axes are defined in Fig. 1. Since the electron and ion current at the anode,  $J_e$  and  $J_i$ , are to be independent of  $x$  and  $y$ , the  $y$  component of the surface current (current per unit width) must be  $\sigma_y = Jy = (J_e + J_i)y$  to conserve current. The magnetic field deep in the anode (i.e., in the anode plasma for a plasma-filled diode or in the anode metal for a metal-dielectric anode<sup>9-11</sup>) is zero so the magnitude of the tangential magnetic field at the anode,  $B_a$ , is given by  $B_a = \mu_0 \sigma_a$ , where  $\sigma_a$  is the magnitude of the surface current. Since  $B_a$  must be independent of position so must  $\sigma_a$ . Therefore

$$\sigma_y^2 + \sigma_x^2 = (Jy)^2 + \sigma_x^2 = \sigma_a^2.$$

The surface current path can then be found from the differential equation

$$\begin{aligned} dy/dx &= \sigma_y/\sigma_x = Jy/[\sigma_a^2 - (Jy)^2]^{1/2} \\ &= (y/b_0)/[1 - (y/b_0)^2]^{1/2}, \end{aligned}$$

where the geometric constant  $b_0$  is given by  $b_0 = \sigma_a/J > b$ . The integral of this equation is

$$x/b_0 = -\ln\{1 + [1 - (y/b_0)^2]^{1/2}\} / (y/b_0) \\ + [1 - (y/b_0)^2]^{1/2} + \text{const.}$$

The magnetic field line projection on the anode surface is normal to the current path and thus given by

$$dy/dx = -\sigma_x/\sigma_y = -[1 - (y/b_0)^2]^{1/2} / (y/b_0)$$

or again by integrating

$$x/b_0 = [1 - (y/b_0)^2]^{1/2} + \text{const.}$$

The field lines at the anode are thus circular with a radius of  $b_0$ .

At this point the currents in the gap could be assumed to be parallel to the surface current in the anode, or the magnetic field could be assumed to be parallel to that at the anode. These assumptions will soon be seen to be equivalent (to order  $S^2$ ). It is convenient to assume that the latter (constant field direction across the diode) which, when combined with  $\vec{\nabla} \cdot \vec{A} = 0$ , gives a general form for the vector potential of

$$A_x = -a(z)[1 - (y/b_0)^2]^{1/2}, \\ A_y = -a(z)(y/b_0), \\ A_z = b_0^{-1} \int_{-\infty}^z a(z) dz, \quad (2.1a)$$

where  $B(-\infty) = 0$  and  $a(z)$  is arbitrary except that  $a(-\infty) = 0$ . The magnetic field is then given by

$$B_x = \frac{\partial A_z}{\partial y} - \frac{\partial A_y}{\partial z} = \frac{da}{dz} \frac{y}{b_0}, \\ B_y = \frac{\partial A_x}{\partial z} - \frac{\partial A_z}{\partial x} = -\frac{da}{dz} \left[ 1 - \left( \frac{y}{b_0} \right)^2 \right]^{1/2}, \\ B_z = \frac{\partial A_y}{\partial x} - \frac{\partial A_x}{\partial y} = \frac{-a(z)}{b_0} \frac{y}{b_0} \left[ 1 - \left( \frac{y}{b_0} \right)^2 \right]^{-1/2}. \quad (2.1b)$$

The current densities are given by  $\mu_0 \vec{j} = \vec{\nabla} \times \vec{B}$  or

$$\mu_0 j_x = \frac{\partial B_z}{\partial y} - \frac{\partial B_y}{\partial z} \\ = \frac{a}{b_0^2} \left[ 1 - \left( \frac{y}{b_0} \right)^2 \right]^{-3/2} \\ + \frac{da^2}{dz^2} \left[ 1 - \left( \frac{y}{b_0} \right)^2 \right]^{1/2}, \\ \mu_0 j_y = \frac{\partial B_x}{\partial z} - \frac{\partial B_z}{\partial x} = \frac{d^2 a}{dz^2} \frac{y}{b_0}, \\ \mu_0 j_z = \frac{\partial B_y}{\partial x} - \frac{\partial B_x}{\partial y} = -\frac{1}{b_0} \frac{da}{dz}. \quad (2.1c)$$

By looking at the dot product of the tangential

$(x, y)$  components of  $\vec{B}$  and  $\vec{j}$ , it is seen that there is a small component of  $\vec{j}$  parallel to  $\vec{B}$ , but that it is down from the normal component by approximately  $ab_0^{-2}(d^2a/dz^2)^{-1}$ , which is of order  $S^2$  since  $b_0 > b$ . Thus the tangential components of magnetic field and diode current density are normal to each other to the order of  $S^2$ , which is necessarily small for small edge effects. It is also clear that the tangential component of the magnetic field is given by

$$B_{||} = (B_x^2 + B_y^2)^{1/2} = \mu_0 b_0 j_z \quad (2.1d)$$

for all values of  $z$ .

The field coil must be designed to give the proper boundary condition at the cathode side of the diode. Electrons flow in from the cathode at the power input side of the diode (Fig. 1) and the net value of  $j_z$  must then be given by  $J_i$ . The  $x$  component of the magnetic field is thus given by  $B_{cx} = \mu_0 J_i y$ . From Eq. (2.1d) the total tangential magnetic field at the cathode is given by  $B_c = \mu_0 J_i b_0$ . The current per unit width at the power feed ( $y = b$ ) is just the current density times the diode height  $b$ , i.e.,  $\sigma_y(b) = Jb$ . If the coil consists of vanes spaced  $\Delta x$  apart in the  $x$  direction, then the current per vane must be  $Jb \Delta x$ . The spacing in  $y$  of the vanes  $\Delta y$  then gives the coil current per unit width in the  $y$  direction  $Jb \Delta x / \Delta y$ . This can be put in Ampere's law to get

$$B_{cy} + B_{dc} = 2\mu_0 Jb \frac{\Delta x}{\Delta y}, \quad (2.2)$$

where  $B_{cy}$  is the  $y$  component at the first cathode and  $B_{dy}$  is the  $y$  component in the drift region between the coil and the second cathode (see Fig. 1). The factor of 2 in Eq. (2.2) is due to the two layers of the field coil. Equation (2.2) can be rewritten

$$B_{cy} = \frac{2}{1 + (B_{dy}/B_{cy})} \mu_0 Jb \frac{\Delta x}{\Delta y}.$$

The flux between the anode and the field coil due to  $B_y$  must be the same as that between the field coil and the second cathode. This is because of the small field penetration into the metal conductors on the time scale of the diodes ( $\sim 30$  ns). The ratio  $B_{dy}/B_{cy}$  must be related to the ratio of the gap between the anode and the field coil to the gap between field coil and second cathode. However, the field at the field coil is not the same as that at the anode so the field ratio is not simply the ratio of the gaps. For the moment the ratio will be assumed to be one. This will be discussed further in Sec. VII. With this assumption then

$$B_{cy} = \mu_0 Jb \frac{\Delta x}{\Delta y} = \mu_0 Jb \frac{dX(y)}{dy},$$

where  $X(y)$  is the vane shape function for the coil and the finite difference has been replaced with a differential since the coil vanes are to be closely spaced so  $\Delta x$  and  $\Delta y$  are small compared to the vane radius of curvature in the  $x, y$  plane. Combining this with  $B_{cx} = \mu_0 J_i y$ ,  $B_c = \mu_0 J_i b_0$ , and  $B_c^2 = B_{cx}^2 + B_{cy}^2$  yields the equation for the vane shape  $X(y)$

$$\frac{Jb}{J_i b_0} \frac{dX}{dy} = \frac{b}{b_0 \eta} \frac{dX}{dy} = \left[ 1 - \left( \frac{y}{b_0} \right)^2 \right]^{1/2}, \quad (2.3a)$$

where  $\eta = J_i / (J_e + J_i)$  is the diode efficiency. Equation (2.3a) is readily integrated to yield

$$\frac{b}{b_0 \eta} X(y) = \frac{1}{2} \left\{ y \left[ 1 - \left( \frac{y}{b_0} \right)^2 \right]^{1/2} + b_0 \sin^{-1} \frac{y}{b_0} \right\}. \quad (2.3b)$$

For  $b_0 = 2b$  (which says that the tangential magnetic field is twice the maximum self-field) the right side of Eq. (2.3a) varies from 1.0 at  $y = 0$  to 0.87 at  $y = b$ . The slope of the coil is then almost a constant and equal to  $b_0 \eta / b$ . For this reason, although both  $b_0 \eta$  and  $b_0$  are involved in the coil design, the design is usually more sensitive to  $b_0 \eta$  than to  $b_0$ .

Thus far the general forms of vector potential and magnetic field which have uniform  $J_e, J_i$  and tangential magnetic field have been found. The vector potential in the anode cathode gap was found using the constancy of the skin current in the anode. The details of this skin current will be considered in Secs. IV and V.

It is convenient to define a new coordinate system in which the fields, potentials, and currents are in simpler form. This system will be called the  $g, h, z$  system, where  $z$  is the same as that in the  $x, y, z$  system. Ignoring for the moment the  $z$  component since it is unchanged, the  $g, h$  system is defined by

$$(x - g) / b_0 = [1 - (y / b_0)^2]^{1/2} \quad (2.4a)$$

and

$$\frac{h - x}{b_0} = \ln \left[ \frac{1 + [1 - (y / b_0)^2]^{1/2}}{y / b_0} \right] - \left[ 1 - \left( \frac{y}{b_0} \right)^2 \right]^{1/2}. \quad (2.4b)$$

Clearly, a constant  $g$  line is a projection of the magnetic field lines on the anode and a constant  $h$  line is a projection of vector potential lines. By adding these two equations it is seen that  $h - g$  is a function of  $y$  and independent of  $x$

$$\frac{h - g}{b_0} = \ln \left[ \frac{1 + [1 - (y / b_0)^2]^{1/2}}{y / b_0} \right]$$

or

$$y / b_0 = \operatorname{sech}[(h - g) / b_0]. \quad (2.4c)$$

To find the metric of the  $g, h, z$  system

$$dg = dx + (y / b_0) [1 - (y / b_0)^2]^{-1/2} dy.$$

$$dh = dx - (y / b_0)^{-1} [1 - (y / b_0)^2]^{1/2} dy,$$

or

$$[1 - (y / b_0)^2]^{1/2} dg = [1 - (y / b_0)^2]^{1/2} dx$$

$$+ (y / b_0) dy,$$

$$(y / b_0) dh = (y / b_0) dx - [1 - (y / b_0)^2]^{1/2} dy.$$

Squaring both of these and adding them and also adding  $dz^2$  yields

$$\begin{aligned} ds^2 &= dx^2 + dy^2 + dz^2 \\ &= [1 - (y / b_0)^2] dg^2 + (y / b_0)^2 dh^2 + dz^2 \\ &= \tanh^2 \left[ \frac{h - g}{b_0} \right] dg^2 \\ &\quad + \operatorname{sech}^2 \left[ \frac{h - g}{b_0} \right] dh^2 + dz^2, \end{aligned} \quad (2.5a)$$

where  $ds$  is the distance element along any path. Since there are no cross terms the system is orthogonal. The unit vectors are easily found to be

$$\begin{aligned} \hat{g} &= \hat{x} \tanh \left[ \frac{h - g}{b_0} \right] + \hat{y} \operatorname{sech} \left[ \frac{h - g}{b_0} \right], \\ \hat{h} &= \hat{x} \operatorname{sech} \left[ \frac{h - g}{b_0} \right] - \hat{y} \tanh \left[ \frac{h - g}{b_0} \right], \end{aligned} \quad (2.5b)$$

and  $\hat{z}$ . The vector potential and field can now be written simply as

$$\vec{A} = -a(z) \hat{g} + \frac{\hat{z}}{b_0} \int_0^z a(z) dz, \quad (2.6a)$$

$$\vec{B} = \frac{da}{dz} \hat{h} - \frac{a(z)}{b_0} \operatorname{csch} \left[ \frac{h - g}{b_0} \right] \hat{z} \quad (2.6b)$$

and the current density in the diode gap is [from Eq. (2.1c)]

$$\begin{aligned} \mu_0 \vec{J} &= \frac{d^2 a}{dz^2} \hat{g} - \frac{\hat{z}}{b_0} \frac{da}{dz} \\ &\quad + \frac{a}{b_0^2} \coth^2 \left[ \frac{h - g}{b_0} \right] \left[ \hat{g} + \hat{h} \operatorname{sech} \left[ \frac{h - g}{b_0} \right] \right]. \end{aligned} \quad (2.6c)$$



Individual electrons are accelerated continually, but the electron cloud as a whole is in equilibrium and is not accelerating toward either electrode. Therefore the total pressure (particle plus field) is the same at both electrodes. Thus, if the voltage across the gap is  $V$ ,

$$\frac{B_a^2}{2\mu_0} = \frac{B_c^2}{2\mu_0} + \frac{J_i}{e} M \left[ \frac{2eV}{M} \right]^{1/2} \quad (3.2)$$

since the electric field is zero at both electrodes (space-charge limited flow), the ion momentum is zero at the anode, and the momentum of electrons lost to the anode is neglected (legitimate for  $\eta^2 \gg m/M$ ). In the above  $M$  is the mass for a singly ionized particle, but in general it is the mass divided by the number of times ionized, i.e.,  $M = m_i/z_i$ . Combining Eqs. (3.1) and (3.2) we have

$$\eta^2(1 + \eta f) = 1, \quad (3.3a)$$

where

$$f = \frac{2\mu_0 J}{B_c^2} \left[ \frac{2MV}{e} \right]^{1/2} = \frac{2}{\mu_0(b_0\eta)^2 J} \left[ \frac{2MV}{e} \right]^{1/2}. \quad (3.3b)$$

This expression gives the efficiency of the diode. It does not give 100% for finite magnetic fields, which is contrary to a common statement about diode efficiency being 100% for fields above some critical value. The expression is, however, consistent with behavior expected when self-fields are considered. The expression  $b_0\eta$  was used in the denominator of  $f$  because it is closely related to the coil design, as was pointed out at the end of Sec. II. The efficiency expression is correct as stated in Eq. (3.3) for all  $b_0$ , but  $b_0\eta$  is not essentially constant for all voltages and currents if  $b_0$  is too close to  $b$ .

The above expression was derived assuming that all electrons drift in from the cathode at the edge of the diode, and none come across from the field coil (Fig. 1). This should be correct from the charge buildup argument given earlier, and is supported by numerical simulation results. If electrons do come straight across from the coil the first expression in Eqs. (3.3) becomes  $\eta^2(1 + \eta f) \leq 1$ , which reduces the efficiency.

Equation (3.1) yields an added meaning to the geometric constant  $b_0$ . The average drift distance along a drift path (constant  $h$  line) for an electron is equal to the electron current per unit width,  $(B_a - B_c)/\mu_0$ , divided by the electron current density, i.e.,

$$\frac{B_a - B_c}{\mu_0 J_e} = \frac{(1 - \eta)B_a}{\mu_0 J_e} = \frac{B_a}{\mu_0 J} = b_0.$$

Therefore  $b_0$  is also the average drift distance of an electron.

Goldstein and Lee<sup>17</sup> have shown that

$$\frac{J_e}{J_i} = \frac{1 - \eta}{\eta} = \frac{\tau_i}{\tau_e},$$

where  $\tau_e$  and  $\tau_i$  are the average times an electron and ion spend in the diode gap. Since ions travel straight across the gap,  $\tau_i$  is dependent mostly on the size of the gap  $Z$  and the diode voltage. The electron lifetime  $\tau_e$  should be proportional to  $b_0$ , however; so high  $b_0$  should give high  $\eta$  as Eq. (3.3) predicts.

It should be emphasized that Eq. (3.3) has not involved orbit calculations but is rather derived from considerations of momentum balance and from space-charge limited conditions at the electrode. Although  $\eta = B_c/B_a$  was derived for the special geometry of Sec. II it can be proven more generally if the electrons move predominantly normal to the electric and magnetic fields. For this reason Eqs. (3.3) (using the expression for  $f$  with  $B_c$ ) may be true locally for all magnetically insulated ion diodes with large width to gap ratios.

#### IV. PLASMA DYNAMICS FOR PLASMA-FILLED DIODES; SINGLE ION SPECIES

In this section an anode which is a cold, collisionless, quiet plasma of finite electron density  $n_0$  and containing a single ion species is assumed. This plasma might be generated by plasma guns and injected into the diode region.<sup>13</sup> Ions are accelerated from the surface of the anode plasma, across the acceleration gap, after which they pass through the first cathode (Fig. 1). At the same time the anode plasma surface moves back with velocity  $u_s = dZ/dt$ . Part of the plasma ions are being removed by the electric field (to provide the ion current) but the plasma surface motion is caused mostly by magnetic pressure. Since the magnetic pressure pushes on the electrons, an electric field develops to transfer the force to the more massive ions. This results in a potential hump at the plasma surface like that shown in Fig. 3. It is convenient to define a precise boundary between the anode plasma and the acceleration gap. This boundary will be defined as the point where  $E = 0$  (Fig. 3), and at this point  $z = 0$ .

The lower portion of Fig. 3 is drawn in the  $g, z$  system. The potential hump temporarily speeds the electrons up while they are in it. Most of the ions are reflected from this potential hump, but a fraction  $\epsilon$  pass over it. All of the electrons are reflected at the peak, and in doing so they step over a distance

$\lambda$  in the direction of wider flow [increased  $W(\xi)$ ]. From Eq. (2.7b) and Fig. 3 their reflected current density is

$$\frac{n_0 e u_s W(\xi)}{W(\xi - \lambda)} = n_0 e u_s e^{-\lambda/b_0}.$$

Since there is no net current or charge in the plasma at  $z = -\infty$ , this electron current density must equal the ion current density  $n_0 e u_s (1 - \epsilon)$  so that

$$(1 - \epsilon) = e^{-\lambda/b_0}. \tag{4.1a}$$

It will be seen later that  $\epsilon \ll 1$ ; thus

$$\epsilon = \lambda/b_0. \tag{4.1b}$$

The ion and electron current densities are then given by (for  $z < 0$ )

$$n_i = \frac{n_0(2 - \epsilon)u_s}{u_{iz}} = \frac{n_0(2 - \epsilon)u_s}{(u_s^2 - 2e\phi/M)^{1/2}}, \tag{4.2a}$$

$$n_e = \frac{n_0(2 - \epsilon)u_s}{u_{ez}} = \frac{n_0(2 - \epsilon)u_s}{(u_e^2 - u_g^2)^{1/2}} = \frac{n_0(2 - \epsilon)u_s \Theta \left[ u_s^2 + \frac{2e\phi}{m} - \left( \frac{ea}{m} \right)^2 \right]}{\left[ u_s^2 + \frac{2e\phi}{m} - \left( \frac{ea}{m} \right)^2 \right]^{1/2}},$$

where  $\Theta$  is the Heaviside unit step function. The tangential current in the plasma (i.e.,  $z < 0$ ) is due to the electrons alone as the magnetic field has virtually no effect on the ions over the thickness of the plasma sheath; so from conservation of canonical momentum in the  $g$  direction ( $E_g = 0$ )

$$\begin{aligned} u_g &= \frac{ea}{m}, \\ J_g &= -n_e e \frac{ea}{m}. \end{aligned} \tag{4.2b}$$

$$\begin{aligned} \frac{1}{2\mu_0} \left( \frac{da}{dz} \right)^2 - \frac{\epsilon_0}{2} \left( \frac{d\phi}{dz} \right)^2 + (2 - \epsilon)n_0 u_s^2 \left\{ m \left[ 1 + \frac{2e\phi}{mu_s^2} - \left( \frac{ea}{mu_s} \right)^2 \right]^{1/2} \Theta \left[ 1 + \frac{2e\phi}{mu_s^2} - \left( \frac{ea}{mu_s} \right)^2 \right] \right. \\ \left. + M \left[ 1 - \frac{2e\phi}{Mu_s^2} \right]^{1/2} \right\} = (2 - \epsilon)n_0 u_s^2 (m + M), \end{aligned} \tag{4.3a}$$

where the constant of integration is determined by the boundary condition at  $z = -\infty$ , i.e.,  $(d\phi/dx) = (da/dz) = \phi = a = 0$ . Going now to the plasma edge ( $z = 0$ )

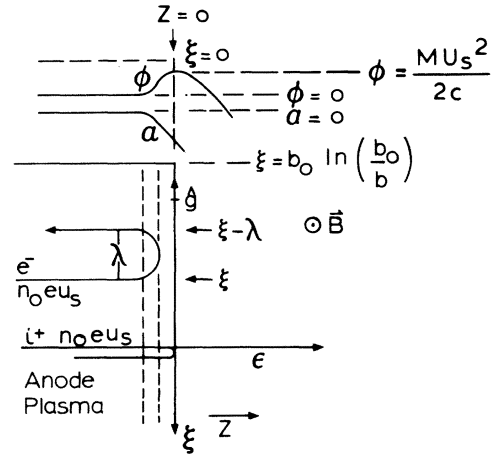


FIG. 3. View of the anode plasma in the rest frame of the plasma surface. Magnetic field pushes on the electrons which then pull on the ions through the electric field on the left side of  $z = 0$ .

By putting Eqs. (4.2a) in Poisson's equation

$$\frac{d^2\phi}{dz^2} = \frac{e(n_e - n_i)}{\epsilon_0} \tag{4.2c}$$

and by multiplying by  $d\phi/dz$ , and by putting Eq. (4.2b) in Ampere's law [Eq. (2.6c)] and multiplying by  $da/dz$ , the equations can be combined and integrated to get the pressure equation

$$\frac{d\phi}{dz} = 0, \quad \phi = \frac{Mu_s^2}{2e}, \quad \left( \frac{ea}{mu_s} \right)^2 \geq 1 + \frac{2e\phi}{mu_s^2},$$

and

$$\frac{da}{dz} = \mu_0 \sigma_0 = \mu_0 b_0 J = \mu_0 b_0 I / A ,$$

where the current is normalized to a finite area  $A$  for later convenience; then from Eq. (4.3a)

$$\frac{\mu_0 b_0^2 I^2}{2A^2} = (2 - \varepsilon)(m + M)n_0 u_s^2 . \quad (4.3b)$$

The single species sheath dynamic constant  $\varepsilon$  is given by (Fig. 3)

$$\varepsilon = \frac{J_i}{n_0 e u_s} = \frac{I \eta}{n_0 e A u_s} \quad (4.4)$$

so

$$\frac{I}{n_0 e A u_s} \left[ \eta + \frac{b_0^2}{2A} \frac{\mu_0 e I}{(m + M) u_s} \right] = 2 . \quad (4.5)$$

It will be seen in Sec. VI that the first  $\eta$  term is always small compared to the second. Therefore, the ratio  $I/u_s$  is virtually constant, i.e., as  $I$  and  $V$  change with time,  $u_s$  changes in proportion to  $I$ .

The relativistic electrons flowing from the cathode into the anode plasma have been neglected in the above calculation. Assuming  $J_i \approx J_e$  (i.e.,  $\eta \approx 50\%$ ) the relativistic electron current density is of the order of  $\varepsilon$  down from  $n_0 e u_s$ . In addition, these electrons are moving at almost the speed of light, so their density is down by  $\varepsilon u_s / c$  from that of the plasma. This is a very small number, typically  $10^{-3}$  to  $10^{-4}$  for systems of interest.

The thickness of the sheath is, of course, calculated by solving Poisson's equation (4.2c) and Ampere's law (2.6c) using Eqs. (4.2a) for the electron and ion densities, and Eq. (4.2b) for the electron current. By normalizing the scalar potential to  $m u_s^2 / 2e$  and the vector potential to  $m u_s / e$ , one finds that the  $d^2 \phi / dz^2$  term of Poisson's equation should be small compared to the  $n_e$  and  $n_i$  terms. This is the common assumption of quasineutrality. Using  $n_e = n_i$  yields

$$\frac{e \phi}{m u_s^2} \left[ 1 + \frac{m}{M} \right] = \left[ \frac{e a}{m u_s} \right]^2 .$$

Using this equation, Ampere's law may be reduced to a second-order differential equation which can be integrated once. The potentials may then be written

$$\frac{e \phi(z)}{m u_s^2} = [F(z/L)]^2 ,$$

$$\frac{e a(z)}{m u_s} = - \left[ \frac{M}{m} + 1 \right]^{1/2} F(z/L) ,$$

where

$$L^2 = \varepsilon_0 m c^2 / [n_0 (2 - \varepsilon) e^2]$$

is the so-called collisionless skin depth and

$$\frac{F'}{[1 - (1 - F^2)^{1/2}]^{1/2}} = 2^{1/2} . \quad (4.6)$$

The magnitude of the  $d^2 \phi / dz^2$ ,  $n_e$ , and  $n_i$  terms of Poisson's equation can be compared *a posteriori*. The first term is found to always be smaller than the other two by  $M u_s^2 / m c^2$ , so the approximation is justified.

Equation (4.6) could easily be integrated numerically. However, it is readily seen that

$$F(x) \simeq e^x , \quad F \ll 1$$

and

$$F(x) \simeq 1 + 2^{1/2} x , \quad F \lesssim 1 .$$

The sheath scale size is thus given by  $L$ .

For  $z > 0$  there are no electrons from the plasma as they cannot cross the magnetic field that far. There will be electrons from the cathode, but that problem is more complex than the present model. For this reason the solution for the potentials in the  $z > 0$  region will be found assuming no electron density, and then an enhancement factor<sup>16,18</sup> will be added to account for electron density in the gap. The magnitude of the enhancement factor may be estimated from the work of Bergeron.<sup>18</sup>

Since electrons are not being considered at the moment, Poisson's equation and Ampere's law are

$$\frac{d^2 \phi}{dz^2} = - \frac{n_0 e u_s}{\varepsilon_0 u_i} = - \frac{I_i}{A \varepsilon_0 (u_s^2 - 2e \phi / M)^{1/2}} ,$$

$$\frac{d^2 a}{dz^2} = 0 .$$

Poisson's equation can be integrated once

$$\frac{\varepsilon_0}{2} \left[ \frac{d \phi}{dz} \right]^2 = \frac{M I_i u_s}{e A} \left[ 1 - \frac{2e \phi}{M u_s^2} \right]^{1/2}$$

and then again to yield

$$I_i = \frac{4A}{9Z^2} \left[ \frac{2e \varepsilon_0^2}{M} \right]^{1/2} \left[ \frac{M u_s^2}{2e} - \phi_c \right]^{3/2} ,$$

where  $\phi_c$  is the cathode potential. Letting  $-\phi_c = V$  (the diode voltage), neglecting  $M u_s^2 / 2e$ , and for instantaneous diode gap  $Z$

$$I_i = \frac{4A}{9Z^2} \left[ \frac{2e \varepsilon_0^2}{M} \right]^{1/2} V^{3/2} .$$

The addition of electrons to the gap region ( $z > 0$ ) will enhance the ion flow.<sup>16,18</sup> This will be taken



$$\mu_1 = \sum_{i=1}^r \frac{M_i \delta_i}{M_r} + \frac{1}{2} \sum_{i=r+1}^N \delta_i \left[ 1 + \frac{M_i}{M_r} \left[ 1 - \left[ 1 - \frac{M_r}{M_i} \right]^{1/2} \right] \right]. \quad (5.6)$$

It will be seen later in Sec. VI that the second term in Eq. (5.5) dominates and, since  $\mu_1 \sim 1$ ,  $\psi$  must be small compared to one. This is because the gap opens mostly due to magnetic pressure rather than ion removal by the electric field.

A Child-Langmuir law is again obtained for the acceleration gap

$$I = \frac{\alpha^2 A}{4\mu_2 \eta} \left[ \frac{2e\epsilon_0}{M_r} \right]^{1/2} \frac{V^{3/2}}{Z^2}, \quad (5.7)$$

where factors for enhancement and electron loss have again been added and the mass factor  $\mu_2$  is

$$\mu_2 = 1 + \psi^{-1} \sum_{i=r+1}^N \delta_i [(M_i/M_r)^{1/2} - 1]. \quad (5.8)$$

Since the various species to be accelerated ( $i = r$  to  $N$ ) will have different velocities there will be multiple ion pulses at the diode focus. The first will be for  $M_r$  and this will generally be the one of interest as it would otherwise be a source of preheat to the target. The source efficiency is therefore defined by (Fig. 4)

$$\eta_s = \frac{\epsilon \delta_r}{\epsilon \delta_r + \sum_{i=r+1}^N \delta_i} = 1 - \psi^{-1} \sum_{i=r+1}^N \delta_i. \quad (5.9)$$

$\psi$  is a small number so the efficiency can be small under some conditions. If  $\eta_s$  appears to be negative, it implies that the value of  $r$  being used is not for the fastest ion in the output and that a higher value of  $r$  should be used. Figure 5 shows  $\eta_s$  vs  $\psi$  for a carbon plasma source developed at Sandia National Laboratories.<sup>19</sup> Assuming a small ion temperature

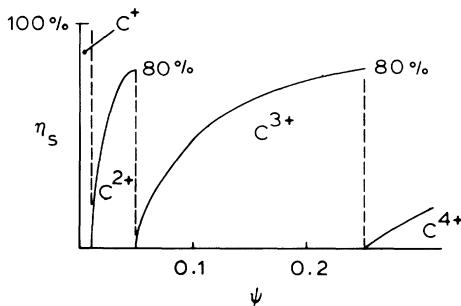


FIG. 5. Source efficiency  $\eta_s$  vs sheath dynamic constant  $\psi$  for a laboratory carbon plasma source.  $\psi$  is typically 0.03 to 0.10.

( $T_i \ll Mu_s^2/2e$ ) would spread the sharp edges of Fig. 5. Poukey<sup>20</sup> has recently confirmed this filtration mechanism with numerical simulations.

## VI. ONE-DIMENSIONAL TIME-DEPENDENT MODEL OF THE PLASMA-FILLED DIODE

A self-consistent one-dimensional configuration for Ampfion diodes has been elaborated above. This will now be used to scale the diode. A simple model will be used for the pulser and diode circuit. This model is shown in Fig. 6. The circuit equation is

$$2U(t) = Z_0 I + L dI/dt + V. \quad (6.1)$$

The model for the diode current is [Eq. (5.7)]

$$I = \frac{\alpha^2}{4\eta\mu_2} \left[ \frac{2e\epsilon_0}{M_r} \right]^{1/2} \frac{AV^{3/2}}{Z^2}.$$

Finally a relationship is needed to get  $Z$ :

$$\frac{dZ}{dt} = u_s = RI, \quad (6.2)$$

where  $R = u_s/I$  is obtained from Eq. (5.5). Since scaling rules are needed the variables are normalized using

$$\begin{aligned} v &= V/U_0, \quad \iota = Z_0 I/U_0, \\ \tau &= t/t_0, \quad \Lambda = L/Z_0 t_0, \\ \xi &= Z_0 Z/RU_0 t_0. \end{aligned} \quad (6.3)$$

The equations then become

$$\begin{aligned} \iota + \Lambda \frac{d\iota}{d\tau} + v &= \begin{cases} 2, & 0 < \tau < 1 \\ 0, & \text{otherwise} \end{cases} \\ \iota &= K v^{3/2} / \xi^2, \\ \frac{d\xi}{d\tau} &= \iota, \end{aligned} \quad (6.4)$$

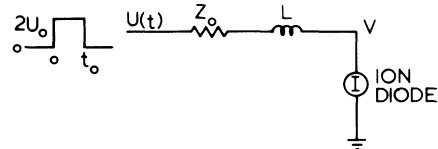


FIG. 6. Circuit model for a diode attached to a transmission line.

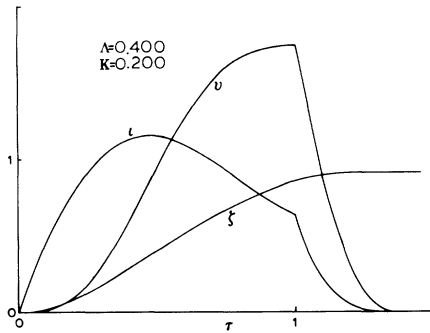


FIG. 7. Normalized diode current  $i$ , voltage  $v$ , and sheath size  $\zeta$  for conditions close to best impedance match to the pulser.

where

$$K = \frac{\alpha^2}{4\eta\mu_2} \left[ \frac{2e\epsilon_0^2}{M_r} \right]^{1/2} \frac{AZ_0^3}{R^2 t_0^2 U_0^{3/2}}. \quad (6.5)$$

Some solutions to Eqs. (6.4) are shown in Fig. 7.

To examine the bunching the time of arrival at the focus (focal length  $f_1$ ) is calculated:

$$T(t) = t + f_1 [2eV(t)/M_r]^{-1/2}. \quad (6.6)$$

This too is normalized:

$$T(t)/t_0 = \tau + \chi v^{-1/2}, \quad (6.7)$$

where

$$\chi = f_1/u_0 t_0, \quad u_0 = (2eU_0/M_r)^{1/2}. \quad (6.8)$$

The optimum values of  $\Lambda$ ,  $K$ , and  $\chi$  are then found by plotting the diode energy  $\int_0^\tau v i d\tau$  versus the time of arrival from Eq. (6.7). Such a plot is shown in Fig. 8. If the diode were 100% efficient, 72% of the energy available to a matched load would arrive at target in  $\frac{1}{4}$  of the power pulse length. The actual energy is down by  $\eta$ . This is a substantial bunching factor.

For this square pulse the parameters  $\Lambda=0.4$ ,  $K=0.2$ , and  $\chi=1.0$  are about optimum. More sophisticated circuits and realistic voltage shapes have been used with this model.<sup>21</sup> The value of  $\chi$  does not seem to be too critical.<sup>22</sup> The values of  $\Lambda$  and  $K$  are adjustable by shimming the series inductor and by adjusting the plasma fill, respectively.

It is now possible to judge the size of the two terms in Eqs. (4.5) and (5.5). For a practical diode  $K$  is of order 1 (see above), the enhancement<sup>18</sup> is presumably of order 1, the efficiency is of order 1, and the mass coefficient is of order 1. In addition,

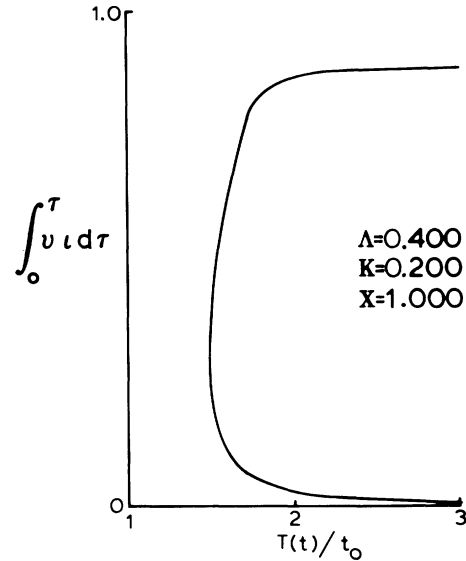


FIG. 8. Diode energy vs time of arrival at focus for normalized focal length 1.0. At any instant  $T$  the energy which has arrived at focus is the difference between the upper and lower branches of this curve.

for reasonable pitch coils,  $b_0$  is of order  $A^{1/2}$ , and for a diode with "f number" about 1 and good bunching (see above),  $A^{1/2}$  is roughly equal to the focal length which is about  $u_0 t_0$  (see above). It is thus readily found that the second term is of order

$$(u_0/c)^{1/2} (\mu_0/\epsilon_0)^{3/4} Z_0^{-3/2}.$$

This is typically about 30 to 100 for diodes of interest. Therefore, from Eqs. (4.5) or (6.5) the  $\eta$  term is negligible and  $I/u_r$  is essentially constant. In addition, since the expression outside the brackets in Eqs. (4.5) and (5.5) are  $\epsilon/\eta$  and  $\psi/\eta$ , respectively, it is clear that  $\epsilon \ll 1$  for the single species case [Eq. (4.5)] and  $\psi \ll 1$  for the multiple species case [Eq. (5.5)].

## VII. DESIGNING A FOCUSING DIODE

From the point of view of diode operation the strip diode model is more than adequate. To drift and focus ions, however, it is necessary to go to a quasispherical diode where the deviation from a true sphere is determined by the magnetic focusing effect.<sup>23,24</sup> The assumption made depends somewhat upon the exact diode being considered. As an example the Ampfion-hybrid diode shown in Fig. 9 will be used. This is an extraction diode using an annular first-cathode electron source. The field coil

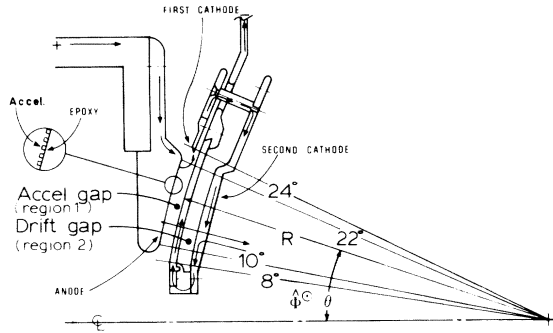


FIG. 9. A section of an Ampfion-hybrid which is built for the Hydramite pulser.  $\theta_i = 10^\circ$  and  $\theta_o = 22^\circ$  are the inner and outer anode angles. Here CL stands for center line. In the experiment, the diode is initially filled with a low density plasma ( $n_e \sim 10^{13} \text{ cm}^{-3}$ ) from the anode to the focal region. This plasma provides a low initial impedance to reduce prepulse and provides field-free ion drift to the focus.

vanes, in addition to providing the radial magnetic field, also supply an equipotential surface on the cathode side of the gap. The ion source used in this diode is a dielectric proton source (grooved aluminum with epoxy fill) and not a dense plasma prefill. A low density plasma fill is generally used to provide field-free ion drift in the drift region. The gap between the anode and the coil and between the coil and second cathode are the same (6 mm). The focal length is about 20 cm and the various angles of field coil and anode are shown in Fig. 9.

First, the pitch of the field coil vanes is calculated. Assuming constant diode current density the current enclosed inside a circle about the axis at the cathode is

$$\frac{\eta IA(\theta)}{A(\theta_0)} = \frac{\eta I(\cos\theta_i - \cos\theta)}{(\cos\theta_i - \cos\theta_0)},$$

where  $\theta$  is the polar angle at the circle,  $\theta_i$  is the polar angle at the inner edge of the anode,  $\theta_o$  is the polar angle at the outer edge of the anode, and  $A(\theta)$  is the area between  $\theta_i$  and  $\theta$ . The efficiency factor  $\eta$  is included since the ion current alone appears at the cathode. The  $\hat{\phi}$  component of the magnetic field at the cathode is then

$$B_{\hat{\phi}} = \frac{\mu_0 I(\theta)\eta}{2\pi R(\theta)\sin\theta} = \frac{\mu_0 I\eta}{2\pi R(\theta)\sin\theta} \frac{\cos\theta_i - \cos\theta}{\cos\theta_i - \cos\theta_0}.$$

The number of vanes in the field coil is  $2\pi/\Delta\phi$ , where  $\Delta\phi$  is the angular spacing between vanes. The current per vane is then  $I\Delta\phi/2\pi$  since the entire diode current runs through the field coil. The spacing between vanes in the theta direction is  $R\Delta\theta$  so the field coil current per unit width in the theta

direction is

$$\frac{I}{2\pi R} \frac{\Delta\phi}{\Delta\theta}.$$

From Ampere's law the theta component of the magnetic field at the first cathode ( $B_{c\theta}$ ) and drift side ( $B_{d\theta}$ ) of the coil are then given by

$$B_{c\theta} + B_{d\theta} = B_{c\theta}(1 + B_{d\theta}/B_{c\theta}) = \frac{\mu_0 I}{2\pi R} \frac{\Delta\phi}{\Delta\theta}.$$

The gaps are the same on both sides of the field coil. The flux must be the same on both sides because no flux can penetrate the anode and second cathode on the 30-ns time scale of the diode pulse. If the magnetic field were constant across the acceleration gap, the average field  $\bar{B}_{\theta} (\propto \text{flux/gap})$  would be equal to  $B_{c\theta}$ . However,  $B_{a\theta} = B_{c\theta}/\eta$  and the average field is between  $B_{a\theta}$  and  $B_{c\theta}$ . This is a good area for further research. For the present calculation the geometric mean of  $B_{a\theta}$  and  $B_{c\theta}$  will be used for the average field. Then

$$B_{\theta} = (B_{a\theta} B_{c\theta})^{1/2} = B_{c\theta}/\eta^{1/2}.$$

The flux and gap are the same on the drift side of the field coil and drifting electrons are neglected since the voltage must be due to the ion space charge and can be only a fraction of the anode voltage. Therefore  $B_{c\theta}/B_{d\theta} = \eta^{1/2}$ . Then

$$B_{c\theta} = \frac{1}{1 + \eta^{-1/2}} \frac{\mu_0 I}{2\pi R} \frac{\Delta\phi}{\Delta\theta}.$$

The total tangential field at the cathode is again  $\mu_0 \eta I b_0 / A$ , so

$$\left[ \frac{\mu_0 \eta I b_0}{A} \right]^2 = B_{\theta}^2 + B_{\hat{\phi}}^2.$$

Letting  $\Delta\phi/\Delta\theta = d\phi/d\theta$

$$\left[ \frac{\mu_0 \eta b_0 I}{A} \right]^2 = \left[ \frac{1}{1 + \eta^{-1/2}} \frac{\mu_0 I}{2\pi R} \frac{d\phi}{d\theta} \right]^2 + \left[ \frac{\mu_0 I \eta}{2\pi R \sin\theta} \frac{\cos\theta_i - \cos\theta}{\cos\theta_i - \cos\theta_0} \right]^2$$

or

$$\begin{aligned} \frac{A}{2\pi b_0 R \eta (1 + \eta^{-1/2})} \frac{d\phi}{d\theta} &= \frac{R(\cos\theta_i - \cos\theta_0)}{(1 + \eta^{-1/2})\eta b_0} \frac{d\phi}{d\theta} \\ &= \left[ 1 - \left[ \frac{R}{b_0} \frac{\cos\theta_i - \cos\theta}{\sin\theta} \right]^2 \right]^{1/2}, \end{aligned} \quad (7.1)$$

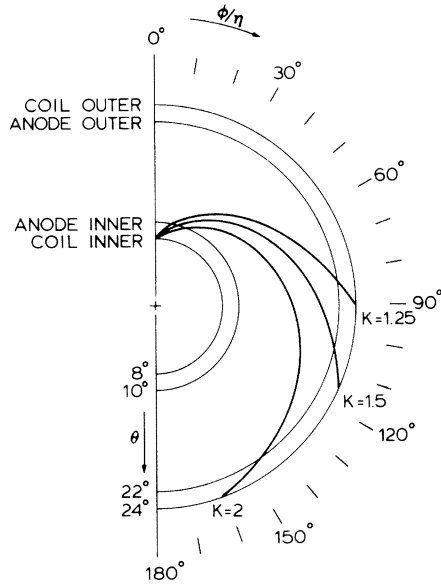


FIG. 10.  $\phi(\theta)$  plot of a field coil vane for three different coil factors  $K_0$ .

where  $A = 2\pi R^2 (\cos\theta_i - \cos\theta_0)$  has been used. For the diode shown in Fig. 9 the right side of Eq. (7.1) varies from 1.0 for  $\theta = \theta_i = 10^\circ$  to 0.9 for  $\theta = \theta_0 = 22^\circ$  so the pitch  $d\phi/d\theta$  is almost independent of  $\theta$  and is about 6. The small variation of  $R(\theta)$  has been neglected in obtaining Eq. (7.1). Equation (7.1) is easily integrated, and the shapes for several  $b_0$  values are shown in Fig. 10. The plots are actual shapes for  $\eta = 1$ . For  $\eta < 1$  the pitch will be lower.

The next calculation will give  $R(\theta)$ . It could be done before the vane figure calculation and used in (7.1). However, variation in  $R$  has a negligible effect on field coil vane design when compared to time-dependent effects and does not seem worthwhile.

The ions are deflected in the acceleration gap (region 1, Fig. 9) and the drift gap (region 2, Fig. 9). To calculate the deflection accurately, the  $B_\phi$  profiles across both gaps need to be calculated. Once again the average  $B_\phi$  in the acceleration gap must be somewhere between the values at the anode and the cathode and the geometric mean of  $B_{a\phi}$  and  $B_{c\phi}$  are used. Then

$$\int B_\phi dx = \bar{B}_\phi d = \eta^{1/2} B_{a\phi} d = \eta^{1/2} \frac{\mu_0 I(\theta) d}{2\pi R \sin\theta},$$

$$I(\theta) = I \frac{\cos\theta_i - \cos\theta}{\cos\theta_i - \cos\theta_0},$$

$$\sin\delta(\theta) = \frac{2Rd}{b_0^2} \frac{(\eta^{1/2} + \eta)(\cos\theta_i - \cos\theta) - (\cos\theta_i - \cos\theta_0)}{f \sin\theta}.$$

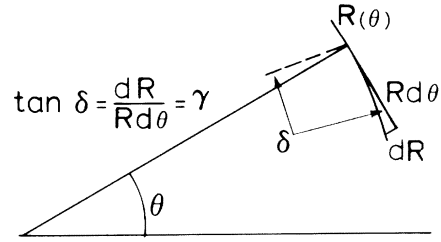


FIG. 11. Relationship between deflection angle  $\delta(\theta)$  and the cathode shape  $R(\theta)$ .

where  $d$  is the diode gap.

In the ion drift side of the coil (region 2, Fig. 9) there will be some drifting fast electrons due to the ion space charge, but they will be neglected. Therefore for the drift-region field  $B_{d\phi}$

$$\int B_{d\phi} dx = \frac{\mu_0 d}{2\pi R \sin\theta} [\eta I(\theta) - I],$$

where the first term is due to ion current and the second is due to current in the center hub which supplies the current to the first and second cathodes.

The transverse velocity is then given by

$$\begin{aligned} v_\perp &= \frac{e}{M} \left[ \int B_\phi dx + \int B_{d\phi} dx \right] \\ &= \frac{\mu_0 e d}{2\pi M R \sin\theta} [I(\theta)(\eta^{1/2} + \eta) - I]. \end{aligned}$$

The total ion velocity is

$$v = \left( \frac{2eV}{M} \right)^{1/2}$$

so the deflection  $\delta(\theta)$  is

$$\begin{aligned} \sin\delta(\theta) &= \frac{v_\perp}{v} \\ &= \frac{\mu_0 d}{2\pi R \sin\theta} \left[ \frac{e}{2MV} \right]^{1/2} [I(\theta)(\eta^{1/2} + \eta) - I]. \end{aligned}$$

Using Eq. (3.3) and

(7.2)

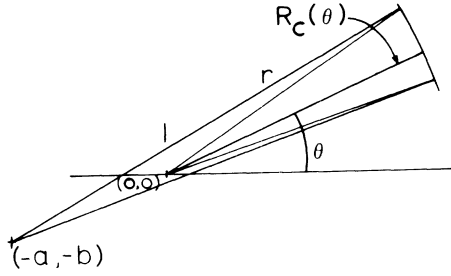


FIG. 12. Offset circular arc used to approximate the ideal  $R(\theta)$ .  $a$  and  $b$  are the axial and radial offsets and  $r$  is the arc radius.  $\theta$  is the polar angle.

The shape of the cathode surface  $R(\theta)$  is then calculated from

$$\tan[\delta(\theta)] = \frac{1}{R} \frac{dR}{d\theta} \equiv \gamma(\theta) \quad (7.3)$$

as can be seen from Fig. 11.

It is easier to machine the anode surface (which conforms to the cathode surface) in the form of an arc of a circle rotated about the axis. The general form of  $R(\theta)$  which fits this shape is

$$r^2 = R_0^2(\theta) + a^2 + b^2 + 2R_0(\theta)(a \cos\theta + b \sin\theta),$$

where a subscript 0 refers to a circular-arc-generated surface (see Fig. 12). Using (7.3)

$$\tan[\delta_0(\theta)] = \gamma_0 = \left[ \left( \frac{r}{a \sin\theta - b \cos\theta} \right)^2 - 1 \right]^{-1/2}$$

which can be rewritten as

$$\sin[\delta_0(\theta)] = \frac{a \sin\theta - b \cos\theta}{r}. \quad (7.4)$$

This can be fit to (7.2) by various methods but, in particular, a mean-square fit can be found analytically.

A function

$$F = \alpha \sin\theta - \beta \cos\theta$$

must be fit to a function  $G(\theta)$ . The mean-square fit  $\rho^2$  is given by

$$\begin{aligned} \rho^2 = \langle (F - G)^2 \rangle = & \alpha^2 \langle \sin^2\theta \rangle + \beta^2 \langle \cos^2\theta \rangle \\ & + \langle G^2 \rangle - 2\alpha\beta \langle \sin\theta \cos\theta \rangle \\ & - 2\alpha \langle G \sin\theta \rangle + 2\beta \langle G \cos\theta \rangle, \end{aligned}$$

where

$$\langle F \rangle \equiv \int_{\theta_i}^{\theta_0} F d\theta / (\theta_0 - \theta_i). \quad (7.5)$$

These averages all consist of integrals of powers of trigonometric functions and are readily done. The best mean-square fit requires minimum  $\rho^2$ . Therefore

$$\frac{\partial \rho^2}{\partial \alpha} = \frac{\partial \rho^2}{\partial \beta} = 0$$

which yields

$$\begin{aligned} \alpha \langle \sin^2\theta \rangle - \beta \langle \sin\theta \cos\theta \rangle &= \langle G \sin\theta \rangle, \\ \alpha \langle \sin\theta \cos\theta \rangle - \beta \langle \cos^2\theta \rangle &= \langle G \cos\theta \rangle, \end{aligned} \quad (7.6)$$

which are readily solved for  $\alpha$  and  $\beta$ . The function  $\sin\delta(\theta)$  from (7.2) is then put in place of  $G$  in (7.6) which then gives the axial and radial offsets  $a$  and  $b$  by  $a/r = \alpha$  and  $b/r = \beta$  for any  $r$ .

The aspheric shape of the cathode surfaces causes the shape of the vanes in the field coils to be noncircular arcs. Their shape is determined by two constraints. (1) They must provide the proper  $R_0(\theta)$  when shaped to the desired  $\phi(\theta)$ . (2) They should be normal to the  $R_0(\theta)$  surface when in place. The latter requirement is to minimize ion loss to the coil vanes by minimizing the projected cross section.

The vanes for this diode are to be cut from shim metal stock. To obtain the vane shape as it is to be cut from the shim stock requires the functions  $R_0(\theta)$  and  $\phi(\theta)$  found earlier in this section.  $\phi$  is the polar angle (colatitude) and  $\theta$  the equatorial angle (longitude). The unit normal to the surface is  $\hat{n}$ , which makes an angle  $\delta(\theta)$  to the radius vector  $r$ . From (7.3) the unit vector  $\hat{n}$  is then

$$\begin{aligned} n_\phi &= 0, \\ n_\theta &= -\sin\delta = -\gamma / (1 + \gamma^2)^{1/2}, \\ n_r &= 1 / (1 + \gamma^2)^{1/2}, \end{aligned} \quad (7.7)$$

where again

$$\gamma = \frac{1}{R} \frac{dR}{d\theta}.$$

The curvature of the vane given by  $R_0(\theta)$  and  $G(\theta) = d\phi/d\theta$  is greater than the curvature normal to the surface. The curvature normal to the surface is needed to find the shape of the vane as it would be cut from flat metal. The curvature of the vane  $\vec{c}$ , is given by

$$\vec{c} = -\frac{d^2\vec{s}}{ds^2}, \quad (7.8)$$

where  $d\vec{s}$  is the vector displacement along the curve  $R(\theta)$ ,  $G(\theta)$ . It can be shown that

$$\begin{aligned} d\vec{s} &= R(\theta) \vec{h}(\theta) d\theta, \quad \vec{h}(\theta) = \hat{\theta} + \gamma \hat{R} + G \sin\theta \hat{\phi}, \\ ds &= R(\theta) h(\theta) d\theta, \quad h(\theta) = (1 + \gamma^2 + G^2 \sin^2\theta)^{1/2}. \end{aligned} \quad (7.9)$$

Combining (7.7) through (7.9), the curvature normal to the surface is found to be

$$\hat{n} \cdot \vec{c} = \frac{1}{R(\theta)} \left[ 1 - \frac{\frac{d\gamma}{d\theta} + G^2(\theta)\sin\theta \cos\theta}{h^2(\theta)} \right]. \quad (7.10)$$

This can then be put equal to the curvature in the plane of the shim stock from which the vane is cut and the actual shape found by solving second-order differential equations.

The radial or  $B_\theta$  field will also bend the ion paths. However, the net flux crossed between anode and second cathode is zero, which says that the vector potential  $A_\phi$  is the same at the anode and second cathode. Conservation of canonical angular momentum about the axis then says that there is no angular momentum after passing the second cathode and the ions can pass through the axis. The focus is only optimized for one instant of time, but temporal variation should be modest if focusing is optimized for peak power.

### VIII. CONCLUSION

It has been shown that an ion diode exists which can be described by a one-dimensional model. Use of this type of diode allows diodes to be designed without extensive computer calculations. In addition,

the diode model provides a qualitative understanding of ion diodes not available in more complicated geometries.

The plasma-filled versions of these diodes are also easily scaled and provide superior impedance matches to conventional transmission lines and particularly to magnetically insulated transmission lines.<sup>14</sup>

Most of the theory presented here has been tested experimentally<sup>13</sup> and good agreement has been found. Work is continuing in two areas. Understanding the behavior of the electrons in these diodes is very important with regard to the actual ion current enhancement and to the self-field deflection of the ions. These effects are being examined analytically and with particle simulations.<sup>15</sup> The development of ion sources for both plasma-filled diodes and surface sources is the most critical area of exploration. Much of this research is empirical as the theory is very complex.

### ACKNOWLEDGMENTS

The author would like to thank J. P. Quintenz and D. B. Seidel for many fruitful discussions on this theory. In addition he would like to thank P. A. Miller, J. R. Freeman, G. W. Kuswa, and, particularly, J. P. Quintenz for critical readings of the manuscript.

- 
- <sup>1</sup>S. Humphries, Jr., R. N. Sudan, and L. Wiley, *J. Appl. Phys.* **47**, 2382 (1976).
- <sup>2</sup>T. M. Antonsen, Jr. and E. Ott, *J. Appl. Phys. Phys. Lett.* **28**, 424 (1976).
- <sup>3</sup>S. J. Stephanakis, D. Mosher, G. Cooperstein, J. R. Bollner, J. Golden, and S. A. Goldstein, *Phys. Rev. Lett.* **37**, 1543 (1976).
- <sup>4</sup>S. Humphries, Jr., *Plasma Phys.* **19**, 399 (1977).
- <sup>5</sup>S. A. Goldstein, G. Cooperstein, R. Lee, D. Mosher, and S. J. Stephanakis, *Phys. Rev. Lett.* **40**, 1504 (1978).
- <sup>6</sup>M. A. Greenspan, D. A. Hammer, and R. N. Sudan, *J. Appl. Phys.* **50**, 3031 (1979).
- <sup>7</sup>J. A. Pasour, R. A. Mahaffey, J. Golden, and C. A. Kapetanakis, *Appl. Phys. Lett.* **36**, 646 (1980).
- <sup>8</sup>R. A. Meger, F. C. Young, A. T. Drobot, G. Cooperstein, S. A. Goldstein, D. Mosher, S. E. Graybill, G. A. Huttlin, K. G. Kerris, and A. G. Stewart, *J. Appl. Phys.* **52**, 6084 (1981).
- <sup>9</sup>D. J. Johnson, G. W. Kuswa, A. V. Farnsworth, Jr., J. P. Quintenz, R. J. Leeper, E. J. T. Burns, and S. Humphries, Jr., *Phys. Rev. Lett.* **42**, 610 (1979).
- <sup>10</sup>D. J. Johnson, A. V. Farnsworth, Jr., D. L. Fehl, R. J. Leeper and G. W. Kuswa, *J. Appl. Phys.* **50**, 4524 (1979).
- <sup>11</sup>S. Humphries, Jr., *Nucl. Fusion* **20**, 1549 (1980).
- <sup>12</sup>C. W. Mendel, Jr., P. A. Miller, J. P. Quintenz, D. B. Seidel, and S. A. Slutz, in *Proceedings of the International Conference on High-Power Electron and Ion-Beam Research and Technology*, edited by H. J. Doucet and J. M. Buzzi, Ecole Polytechnique, Palaiseau, France, July 1981, p. 45.
- <sup>13</sup>C. W. Mendel, Jr. and G. S. Mills, *J. Appl. Phys.* **53**, 7265 (1982).
- <sup>14</sup>G. W. Kuswa, J. P. Quintenz, D. B. Seidel, D. J. Johnson, C. W. Mendel, Jr., E. J. T. Burns, D. Fehl, R. J. Leeper, F. C. Perry, P. A. Miller, M. M. Widner, and A. V. Farnsworth, Jr., in *Proceedings of the International Conference on High-Power Electron and Ion-Beam Research and Technology* (see Ref. 12), p. 3.
- <sup>15</sup>J. P. Quintenz (private communication).
- <sup>16</sup>Thomas P. Antonsen, Jr. and Edward Ott, *Phys. Fluids*, **19**, 52 (1976).
- <sup>17</sup>S. A. Goldstein and R. Lee, *Phys. Rev. Lett.* **35**, 1079 (1975).

<sup>18</sup>Kenneth D. Bergeron, *Appl. Phys. Lett.*, 28, 306 (1976).

<sup>19</sup>G. S. Mills (private communication).

<sup>20</sup>J. W. Poukey (private communication).

<sup>21</sup>D. B. Seidel, J. P. VanDevender, and C. W. Mendel, Jr., *1981 IEEE International Conference on Plasma Science Conference Record, May 1981, Santa Fe, New Mexico* (IEEE, New York, 1981).

<sup>22</sup>S. A. Slutz (private communication).

<sup>23</sup>Stanley Humphries, Jr., *Plasma Phys.*, 19, 399 (1977).

<sup>24</sup>D. Mosher, G. Cooperstein, and Shyke Goldstein, *Technical Digest, Topical Meeting on Inertial Confinement Fusion, San Diego, California, 1980* (Optical Society of America, Washington, D.C. 1980).